

# Theoretical Analysis and Experimental Study on the Influence of Magnet Structure on Sealing Capacity of Magnetic Fluid Seal

Yanhong Cheng, Zhongzhong Wang, and Decai Li\*

Beijing Jiaotong University, No.3 Shangyuancun Haidian District Beijing, P. R. China

(Received 2 April 2018, Received in final form 16 August 2019, Accepted 27 August 2019)

The Magnetic fluid is a new type of magnetic material. It is a colloidal liquid made of nanoscale ferromagnetic particles suspended in a carrier fluid. Magnetic fluid sealing is one of the most successful applications of the magnetic fluid. As a new type of seal with the advantages of no leakage, long life and high reliability, magnetic fluid seal has been widely used under vacuum and low pressure differential condition. Two types of permanent magnets, the annular permanent magnets and the cylindrical magnets, are usually used in magnetic fluid seals in engineering. However, the influence of permanent magnet structure on sealing capacity was not clear, hence a new experimental setup was designed in order to study the influence of permanent magnet structure on sealing capacity. The annular permanent magnets and the cylindrical magnets were used as the magnetic source of the experimental setup in a series of tests respectively. The relationship between the sealing capacity of magnetic fluid seal and the end-face area, axial length of the magnet was analyzed by the electromagnetism theories and theoretical derivation. The result of the experiments shows that the sealing capability grows with the end-face area of the magnet, and the growth rate becomes much slower when magnet end-face area attains a certain value; the reluctance of pole pieces and shaft can't be ignored when magnetic field attains a certain value; the modified theoretical formula had a good match to the measured values when the end-face area of the magnet is small enough to ignore the reluctance of pole pieces and shaft.

**Keywords :** Magnetic fluid, Magnetic fluid seal, Sealing capacity, Permanent magnet structure, Magnetic fluid seal design

## 1. Introduction

Magnetic fluid is a new type of magnetic material [1, 2]. It is a colloidal liquid made of nanoscale ferromagnetic particles suspended in a carrier fluid [3-5]. Magnetic fluid sealing is one of the most successful application of the magnetic fluid [6-8]. The magnetic fluid seals play an important role in the engineering field for they have the advantages of no leakage, high reliability and long life [9, 10].

Two types of permanent magnets, the annular permanent magnets and the cylindrical magnets, are usually used on magnetic fluid seals in engineering [11-13]. The sealing effect of magnetic fluid seal with the annular permanent magnets is better than the cylindrical magnets [14-16]. However, the cylindrical magnets with the advantages of low prices, applied universally, easy batch production are

widely used in engineering application, although the research on the influence of permanent magnet structure on sealing capacity of magnetic fluid seal is not complete.

The total sealing capability of the multistage magnetic fluid seals can be approximately expressed as [2, 3]

$$\Delta p_i = \int_{H_{i\min}}^{H_{i\max}} \mu_0 M dH \approx M_s (B_{i\max} - B_{i\min}) \quad (1)$$

$$\Delta p = \sum_{i=1}^N \Delta p_i \quad (2)$$

Where  $H_{i\min}$  and  $H_{i\max}$  are the minimum and maximum magnetic field strengths under the  $i$  pole tooth, respectively,  $\mu_0$  is the permeability of vacuum,  $M$  is the magnetization of magnetic fluid,  $M_s$  is the saturation magnetization of magnetic fluid,  $N$  is the amount of pole teeth,  $B_{i\max}$  is the maximum magnetic flux density under the  $i$  pole tooth and  $B_{i\min}$  is the minimum magnetic flux density under the  $i$  pole tooth. The magnetic flux density under pole teeth plays a very important role in sealing capability. So, the calculation of magnetic field is the key to analyze the

©The Korean Magnetism Society. All rights reserved.

\*Corresponding author: Tel: +86-010-51684006

Fax: +86-010-51684006, e-mail: dcli@bjtu.edu.cn

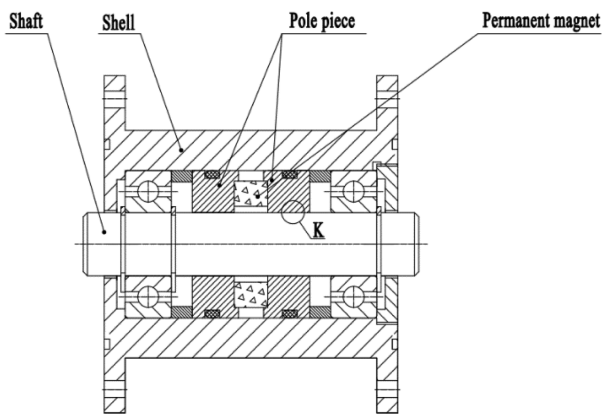
influence of magnet structure on pressure capability.

Analytical method, graphic method, numerical method can be used to calculate the magnetic field. For example Ravaud. R *et al.* [16] calculated the magnetic field of magnetic fluid seal by using complex analysis methods. Mulukutla. S *et al.* [17] and Fan *et al.* [18] calculated the magnetic field in magnetic fluid seal by numerical solutions. Software package Comsol [19] and ANSYS [10] are commonly used in numerical solutions.

However, the above mentioned methods are not universal. The calculation of each sealing device need to restart every step. This paper derived the relationship between the magnetic field and the magnet size by simplifying the magnetic circuit. Furthermore, a series of experiments were done in order to verify the influence of permanent magnet structure on sealing capacity of magnetic fluid seal.

## 2. Experimental Setup

The model seal constructed for the present series of tests is shown in Fig. 1. It consists of a shaft, two pole pieces, a permanent magnet and a shell. The material of



1. Shaft, 2. Pole piece, 3. Permanent magnet, 4. Shell

Fig. 1. Structure of model seal.

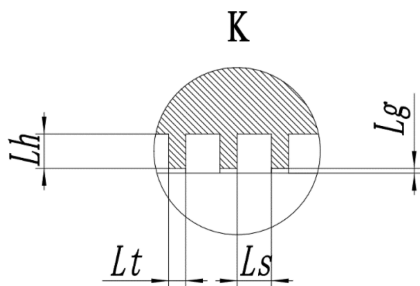


Fig. 2. Local amplification diagram of K.

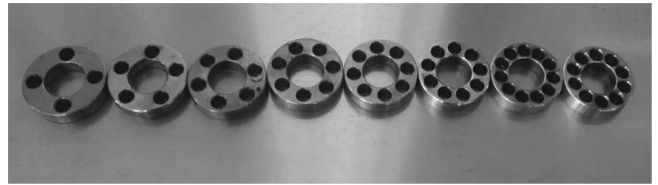


Fig. 3. Cylindrical ring.

the permanent magnet is Nd-Fe-B. The material of the pole pieces and the shaft is 2Cr13 stainless steel. The shell is made of 304 stainless steel. The magnetic fluid used in the current experiment is the engine oil-based magnetic fluid.

In this design, the seal gap  $L_g = 0.1$  mm, the tooth width  $L_t = 0.5$  mm, the tooth height  $L_h = 1$  mm, the clearance between two teeth  $L_s = 1$  mm. Each pole piece have six teeth. The seal gap and the shape of the pole teeth are shown in Fig. 2.

Two shapes of permanent magnets, the annular permanent magnet and the cylindrical magnets, was used in this experiment. Both the annular magnet and the cylindrical magnets were made of the same material with the same height. Cylindrical ring shown in Fig. 3 was produced to ensure the cylindrical magnet circumferentially equispaced on the cylindrical surface of the pole pieces. The inner and outer diameters of the cylindrical ring for placing the plural cylindrical magnets are identical to those of the annular permanent magnet.

The heart of the device is shown in the schematic of Fig. 4. There were, as shown, one end of the seal device connects to the pressure chamber while the other end exposes to the atmosphere. Gas manometer measured the pressure of the pressure chamber. Nitrogen was used as the pressurizing fluid.

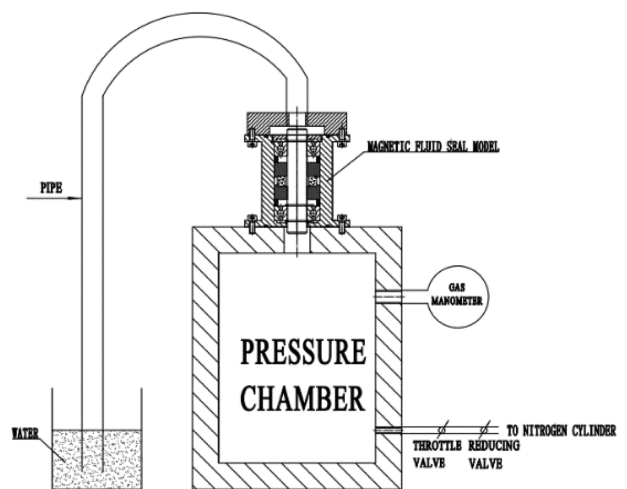


Fig. 4. Schematic of the experimental device.

### 3. Theoretical Calculation of Sealing Capacity

Equivalent magnetic circuit of the magnetic fluid seal used in the experiment is shown in Fig. 5 (the magnetic flux leakage was ignored). Magnetic circuit is conducted by the permanent magnet, pole piece and shaft with good permeability properties and magnetic fluid in the gap between pole teeth and shaft.

The pole pieces on both sides of the magnet are identical, that is,  $R_1 = R_2, R_3 = R_4, R_5 = R_6$ .

According to the ampere's circulation theorem of magnetic field intensity,

$$\oint_L H \cdot dl = \sum_S I_0 \quad (3)$$

It means the line integral of the tangential component of the magnetic field intensity  $H$  around a closed contour  $L$  is equal to the sum of conduction currents  $I_0$  passing through any surface  $S$  linking that contour. There is no conduction current in magnetic fluid seal.

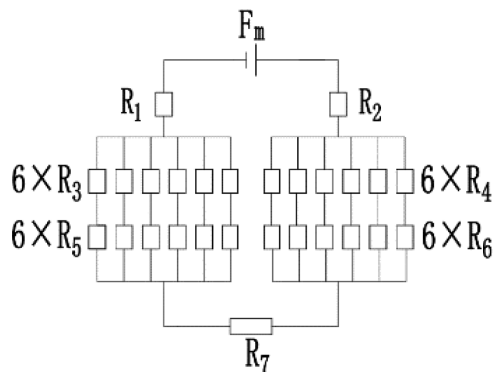
Therefore,

$$\oint_L H \cdot dl = 0 \quad (4)$$

Namely,

$$H_m L_m = 2H_1 L_1 + 2H_3 L_3 + 2H_5 L_5 + H_7 L_7 \quad (5)$$

Where,  $H_m$  and  $L_m$  are the magnetic field intensity and the length of the permanent magnet,  $H_1$  and  $L_1$  are the magnetic field intensity and the length of the magnetic circuit of each pole piece,  $H_3$  and  $L_3$  are the magnetic field intensity and the length of the magnetic circuit of each pole tooth,  $H_5$  and  $L_5$  are the magnetic field intensity and the length of the magnetic circuit of the magnetic



$F_m$ -magnetic potential of magnet,  $R_1, R_2$ -reluctance of the pole pieces,  $R_3, R_4$ -reluctance of the pole tooth,  $R_5, R_6$ -reluctance of the magnetic fluid,  $R_7$ -reluctance of the Shaft

Fig. 5. Equivalent magnetic circuit of the seal.

fluid under each pole tooth,  $H_7$  and  $L_7$  are the magnetic field intensity and the length of the magnetic circuit of the shaft.

The following hypotheses are made:

1. Ignore the magnetic flux leakage in the magnetic circuit of the magnetic fluid seal.

The relative permeability of the shaft and the pole pieces is generally 100-1000 times bigger than air.

2. Ignore edge effect of magnetic fluid in the sealing gap.

3. Ignore the reluctance of the shaft, the pole pieces and the pole tooth to the magnetic field.

The following example would testify that the reluctance of shaft, pole pieces and pole tooth can be ignored. The reluctance of pole tooth is much larger than shaft and pole pieces. Than we just need to compare the reluctance of pole tooth and magnetic fluid.

According to the gauss theorem of the magnetic field,

$$\oiint_s B \cdot dS = 0 \quad (6)$$

Apply it in the magnetic circuit of magnetic fluid seal,

$$B_1 S_1 = 6B_3 S_3 = 6B_5 S_5 = B_7 S_7 = B_m S_m \quad (7)$$

Where,  $B_1$  and  $S_1$  are the average magnetic induction intensity and the area of the pole piece,  $B_3$  and  $S_3$  are the average magnetic induction intensity and the area of each pole tooth,  $B_5$  and  $S_5$  are the average magnetic induction intensity and the area of the magnetic fluid under each pole tooth,  $B_7$  and  $S_7$  are the average magnetic induction intensity and the area of the shaft,  $B_m$  and  $S_m$  are the average magnetic induction intensity and the area of the permanent magnet.

In this magnetic fluid seal model,

$$6S_3 = 6S_5 = \frac{S_1}{3} \quad (8)$$

Therefore,

$$B_3 = B_5 = 3B_1 \quad (9)$$

Normally the magnetic induction intensity in the sealing gap of magnetic fluid seal can reach 1T. Thus,

$$B_3 = B_5 = 1T$$

$$B_1 = 0.33T$$

The magnetic fluid in the sealing gap generally stays in a state of magnetic saturation, its relative permeability approximately equals to the air.

$$H_5 = \frac{B_5}{\mu_0} = \frac{1}{4\pi \times 10^{-7}} = 7.9 \times 10^5 \text{ A/m}$$

The material of the pole pieces and the shaft is 2Cr13 stainless steel. According to the hysteresis loop, that is,  $B$ - $H$  curve of the 2Cr13 stainless steel.

$$H_3 = 576 \text{ A/m}$$

And,  $L_3 = 1 \text{ mm}$ ,  $L_5 = 0.1 \text{ mm}$ ,

$$\frac{H_3 L_5}{H_3 L_3} = 1.37 \times 10^2$$

The value of the third item is much larger than other items on the right side of equation (5), so the reluctance of the shaft, the pole pieces and the pole tooth to the magnetic field could be ignored.

$$H_m L_m = 2H_5 L_5 \tag{10}$$

Simultaneous equation (7), (10) and  $B_5 = \mu_0 H_5$ ,

$$H_m = 2H_5 L_5 / L_m \tag{11}$$

$$B_m = 6B_5 S_5 / S_m = 6\mu_0 H_5 S_5 / S_m \tag{12}$$

The material of the permanent magnet used in this sealing model is Nd-Fe-B. The demagnetization graph of Nd-Fe-B is approximately in shapes of line. The equation of the demagnetization graph can be expressed as

$$\frac{B - B_r}{0 - B_r} = \frac{H - 0}{-H_c - 0} \tag{13}$$

Where,  $B_r$ ,  $H_c$  is the remanence and coercivity of the Nd-Fe-B.  $H_c$  tooks the absolute value here.

Apply equation (11), (12) in (13)

$$H_5 = \frac{H_c B_r}{\left(\frac{6\mu S_5}{S_m} H_c - \frac{2L_5}{L_m} B_r\right)} \tag{14}$$

$$B_5 = \frac{\mu_0 H_c B_r}{\left(\frac{6\mu S_5}{S_m} H_c - \frac{2L_5}{L_m} B_r\right)} \tag{15}$$

Assume  $B_{i \min} = 0$ .

Apply equation (14), (15) in (1) and (2):

$$\Delta p = \frac{12 \cdot M_s \mu H_c B_r}{\left(\frac{6\mu S_5}{S_m} H_c - \frac{2L_5}{L_m} B_r\right)} \tag{16}$$

For common seal,

$$\Delta p = \frac{\mu N M_s H_c B_r}{\left(\frac{N\mu S_5}{2S_m} H_c - \frac{2L_5}{L_m} B_r\right)} \tag{17}$$

### 4. Experiment Process

The experiment procedure is as follows.

First, magnetic fluid was injected in the pole piece by means of a hypodermic needle. And the magnetic fluid volume injected into the stage is sufficient. The permanent magnet between two pole pieces was an annular permanent magnet.

The next step is to install the sealing device and then inject the nitrogen into the sealing chamber slowly by controlling the valve. Record the reading of gas pressure gauge when seal failure occurs. The reading of gas pressure gauge is actually the sealing capability at this moment. Seal failure could be judged by the phenomenon, which is, the continuous emission of gas bubbles in the beaker accompanied by pressure dropping of the sealing chamber. The shaft was static during the whole process of the experiment.

After the steps above was completed, experiment device was cleaned by kerosene which will bring out a good effect.

Replace the annular permanent magnet with eleven cylindrical magnets circumferentially equispaced on the cylindrical surface of pole pieces and then the same steps were re-conducted.

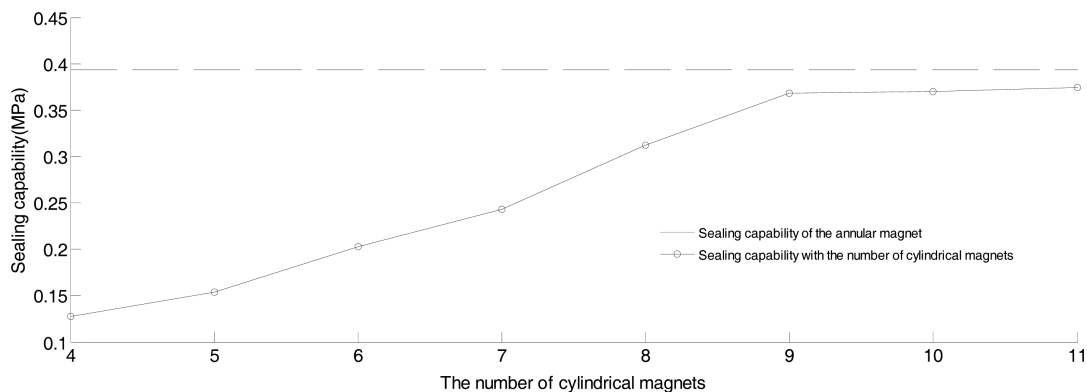


Fig. 6. The changes of sealing capability with cylindrical magnets numbers.

And then, four to ten cylindrical magnets were used as the magnetic source of the experimental setup respectively. Others repeat the above steps.

### 5. Results and Discussion

Fig. 6 shows the experimental results for the changes in sealing capability with the numbers of the magnet. The dashed represents the variation in the sealing capability for the seals using the annular magnet, and the sealing property remains a constant. The solid line represents the change in the sealing capability with the numbers of cylindrical magnets. When the magnet number is less than nine, the sealing capability increases significantly with the magnet numbers. The sealing capability slowly increases when the magnet number exceeds nine. In addition, the sealing capability of using the cylindrical magnet is infinitely close to but smaller than that of using annular magnet when the number of cylindrical magnet is sufficient.

Fig. 7 shows the changes of sealing capability with the end-face area of magnets. As shown, different end-face

areas of the permanent magnets correspond to the different numbers of cylindrical permanent magnets and the annular permanent magnet in Fig. 6. The first eight points of each curve represent the relationship of sealing capacity with different end-face areas of a magnet structure consisting of different numbers of cylindrical magnets. The last point of each curve represents the sealing capacity for the end-face area of the annular permanent magnet. It can be seen that the theoretical sealing capability is larger than measured values. Because the magnetic flux leakage and the reluctance of pole pieces, shaft was ignored and  $B_{i\min} > 0$ . When end-face area of magnets attained a certain value, the reluctance of pole pieces and shaft had a big growth and it can't be ignored. Therefore, the theoretical sealing capability is much larger than the measured values when end-face area attained a certain value.

The theoretical sealing capability growth rate with the magnet end-face area is bigger than experimental value, and this phenomena was much obvious when the end-face area is larger than  $2.54 \times 10^{-3} \text{ m}^2$ , obtained when the number of magnets is nine. When the end-face area was less than  $2.54 \times 10^{-3} \text{ m}^2$ , the experimental sealing cap-

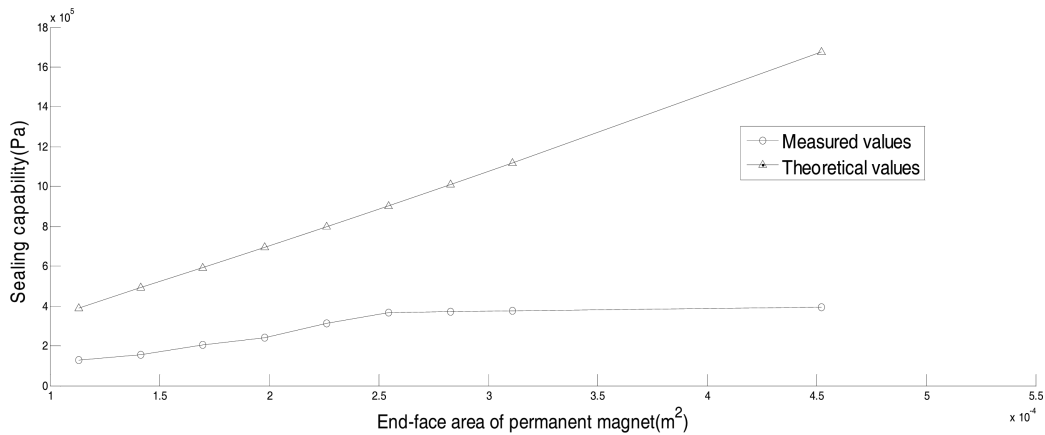


Fig. 7. The changes of sealing capability with the end-face area of magnets.

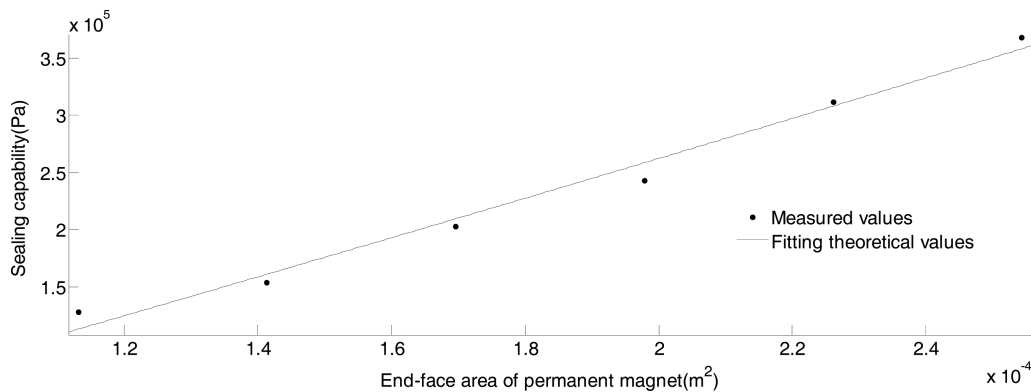


Fig. 8. The sealing capacity of the fitting theoretical values and measured values.

ability growth trend with the area was roughly the same as the theoretical one.

Theoretical formula (16) could be amended by adding a constant term.

$$\Delta p = K \frac{12 \cdot M_s \mu H_c B_r}{\left( \frac{6 \mu S_s}{S_m} H_c - \frac{2 L_s}{L_m} B_r \right)} + C \quad (18)$$

Fitting formula of the measured values could be gotten and the fitting result could be seen in Fig. 8.

$$\Delta p = \frac{7.73 \cdot M_s \mu H_c B_r}{\left( \frac{6 \mu S_s}{S_m} H_c - \frac{2 L_s}{L_m} B_r \right)} - 73450 \quad (19)$$

## 6. Conclusion

(1) The sealing capability grows with the end-face area of magnets, and the growth rate becomes much slower when magnet end-face area attains a certain value.

(2) The reluctance of pole pieces and shaft can't be ignored when magnetic field attains a certain value.

(3) The modified theoretical formula had a good match to the measured values when the end-face area of the magnet is small enough to ignore the reluctance of pole pieces and shaft.

## Acknowledgements

Supported by the Fundamental Research Funds for the Central Universities (No. M19JB400040 and No. M19JB100100).

## References

[1] D. C. Li, The theory and application of magnetic fluid,

Science Press, Beijing (2003) (in Chinese)

- [2] D. C. Li, The theory and application of magnetic fluid seals, Science press, Beijing (2010) (in Chinese)
- [3] S. H. Zhang, Physics of University: Electromagnetics, Tsinghua University Press, Beijing (1999) (in Chinese)
- [4] R. Williams and H. Malsky, Magn. IEEE Trans. **2**, 379 (1980).
- [5] Rosensweig, Ferrohydrodynamics, Cambridge University Press, 1985.
- [6] C. Rinaldi, A. Chaves, S. Elborai, X. T. He, and M. Zahn, Current Opinion in Colloid & Interface Science **3**, 141 (2005).
- [7] Y. Mitamura, S. Arioka, D. Sakota, K. Sekine, and M. Azegami, Journal of Physics Condensed Matter an Institute of Physics Journal. **20**, 204145 (2008).
- [8] O. Pinkus, ASLE Trans. **1**, 79 (1982).
- [9] H. N. Zhang and D. C. Li, Key Eng. Mater. **492**, 273 (2012).
- [10] Z. Z. Wang and D. C. Li, International Journal of Applied Electromagnetics & Mechanics **1**, 101 (2015).
- [11] X. L. Yang, D. C. Li, W. M. Yang, F. F. Xing, and Q. Li, Chinese Journal of Vacuum Science & Technology **1**, 90 (2012).
- [12] X. L. Yang, Z. L. Zhang, and D. C. Li, Science China Technological Sciences **11**, 2865 (2013).
- [13] C. Q. Chi, The basic and applied physics of ferrofluid, Beihang University Press, Beijing (2003) pp. 172-187.
- [14] J. Walowit and O. Pinkus, ASLE Trans. **4**, 533 (1981).
- [15] R. E. Rosenswei, Ferrohydrodynamics, Dover Publications, New York (2002) pp. 54-61&142-146.
- [16] R. Ravaud, G. Lemarquand, and V. Lemarquand, J. Appl. Phys. **3**, 818 (2009).
- [17] M. Sarma, P. Stahl, and A. Ward, J. Appl. Phys. **6**, 2595 (1998).
- [18] Y. G. Fan, F. Y. Chen, and B. Chen, Advanced Materials Research **156-167**, 1097 (2010).
- [19] A. Radionov, A. Podoltsev, and A. Zahorulko, Procedia Engineering **11**, 327 (2012).